Chapter 2

Calorimetry Methods

2.1 Introduction to Calorimetry

Calorimetry is the science of the measurement of heat (from latin, *calor* - 'heat' and *metria* - 'measurement'), typically from chemical reactions, physical changes or phase transitions. Calorimetry is at the heart of most publications that have reported experimental measurements of LENR. In the absence of a cohesive theoretical underpinning of LENR it makes sense to measure the quantity that we care the most about from a practical perspective: heat. This measurement should answer the question whether the heat output exceeds the energy input, as reported in many LENR papers. While calorimetry is agnostic to the mechanism that produces the heat (chemical, nuclear or otherwise), its limitation is that a fairly large number of nuclear events are required in order to be above the sensitivity threshold of a conventional calorimeter, even if each single event releases more energy than a chemical reaction (e.g., > 1000 kJ/mol).

2.2 Concept of Open and Closed System Calorimetry

To perform calorimetry on an electrochemically loaded palladium hydride sample in situ, a typical electrolytic cell, consisting of a palladium cathode and a platinum anode residing in electrolyte, is operated inside the calorimeter. Application of a continuous electrochemical bias is critical to maintain high loading of the palladium hydride. Operating this electrolytic cell above the water splitting voltage will create hydrogen gas and oxygen gas (oxyhydrogen). Depending on the design of the calorimeter, the gas is a) allowed to escape or b) contained within the calorimeter and reverted back into water using a recombiner. Scenario a) is referred to as *(thermodynamically) open calorimetry* and scenario b) is referred to as *(thermodynamically) closed calorimetry*.

In open calorimetry, the chemical energy of the escaping oxyhydrogen gas must be accounted for in the heat balance, while in closed calorimetry, a recombiner must be deployed that reliably and constantly converts oxyhydrogen to water.

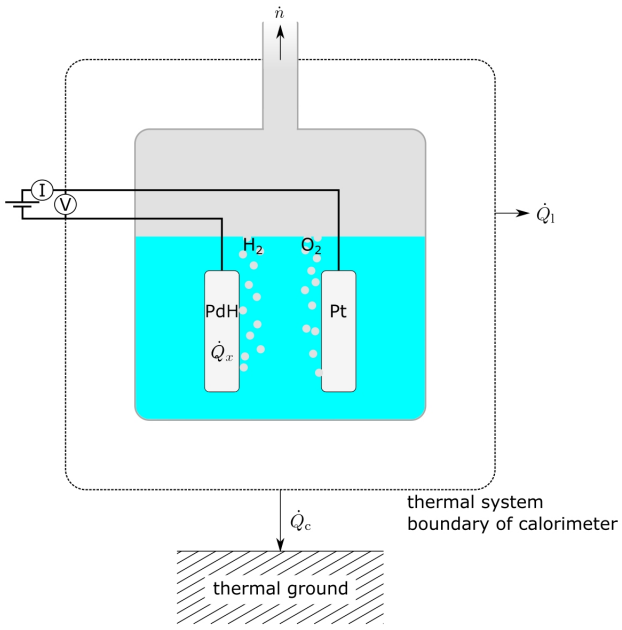

Fig. 2.1: Schematic illustration of an open system calorimeter. $\dot{Q}_x$, heat sources or sinks to be identified, often referred to as *excess heat* in the literature; $\dot{Q}_c$, heat measured by the calorimeter; $\dot{Q}_l$, heat losses escaping measurement by the calorimeter; $\dot{n}$, oxyhydrogen gas stream leaving the system

2.3 Open System Calorimetry

Open system calorimetry is widely used in the LENR research community due to its simplicity and safety (Fig. 2.1). Owing to the open nature of the system, electrochemical experiments are carried out at ambient pressure. There is little risk of potentially dangerous buildup of oxyhydrogen. As a downside, the energy balance is complicated by the fact that the chemical energy of the species leaving the system has to be accounted for. Furthermore, the system is never in steady state, as the electrolyte level changes over time. For the sake of measurement accuracy, if a system is not in steady state, its dynamic behavior, such as the ability of its thermal mass (heat capacity) to absorb or discharge heat, has to be accounted for in the heat balance. A simplified power balance for the open electrochemical system is:

$$|EI| - \dot{Q}_x = \dot{Q}_c + \dot{Q}_l - \dot{n}\Delta H_f \tag{2.1}$$

with

- E, the voltage applied to the electrochemical system measured at the thermal system boundary [V]
- I, the electrolysis current [A]
- $\dot{Q}_x$, the heat sources or sinks to be identified, often referred to as *excess heat* in the literature [W]
- $\dot{Q}_c$, the heat measured by the calorimeter [W]

- $\dot{Q}_\mathrm{l}$, heat losses escaping measurement by the calorimeter[W]
- $\dot{n}$, the oxyhydrogen gas stream leaving the system [mol/s]
- ΔH_f, the formation enthalpy of liquid water, -286 kJ/mol.

The gas flow $\dot{n}$ leaving the system can be measured using a flowmeter, or it can be computed:

$$\dot{n} = \frac{\eta_\mathrm{F} I}{2F} \tag{2.2}$$

with η_F being the Faradaic efficiency and F being the Faraday constant ($9.65 \cdot 10^4$ C/mol). Alternatively, to account for the chemical energy of the oxyhydrogen leaving the system, one can subtract the thermoneutral potential from the applied voltage, assuming that $\eta_\mathrm{F} = 1$. The Faradaic efficiency, η_F, is typically close to 1 for current densities > 150 mA/cm^2 [98, 99].

Due to these and other assumptions built into open system calorimetry, we found them to be particularly susceptible to producing erroneous indications of excess heat.

2.4 Closed System Calorimetry

In a closed system, a recombiner is needed to revert the oxyhydrogen back to water (Fig. 2.2). Thus, there are no mass flows across the thermal system boundary and the power balance simplifies to:

$$EI + \dot{Q}_x = \dot{Q}_\mathrm{c} + \dot{Q}_\mathrm{l}. \tag{2.3}$$

Typically, a platinum catalyst with a large surface area is used as recombiner, e. g., platinum black [100]. We used platinum coated carbon cloth with a platinum loading of 4 mg/cm^2 and a high specific surface area (fuelcellstore.com, item 72500514). If the recombiner works perfectly, and neglecting the pressure buildup due to the generation of 'orphaned' oxygen when the sample is initially loaded with hydrogen, the pressure in the system will remain at ambient. If the sample mass is not negligible, the orphaned oxygen pressure p will go up slightly, depending on the headspace volume V_h compared to the sample mass m_Pd and the loading x_H:

$$\Delta p = \frac{x_\mathrm{H} m_\mathrm{Pd} RT}{2 M_\mathrm{Pd} V_\mathrm{h}}, \tag{2.4}$$

with M_Pd being the molar mass of palladium. In practice, the recombiner might need a certain overpressure to work. We found this to be the case in particular when the recombiner surface is contaminated, e. g., with an electrolyte layer or with salt deposits from the electrolyte. In that case, the vessel pressure goes up and chemical energy Q_p is stored in the headspace as well as pressure-volume work Q_pV :

$$Q_\mathrm{p} = \frac{2 \Delta p V_\mathrm{h} \Delta H_\mathrm{f}}{3RT} \tag{2.5}$$

$$Q_\mathrm{pV} = \Delta p V_\mathrm{h} \tag{2.6}$$

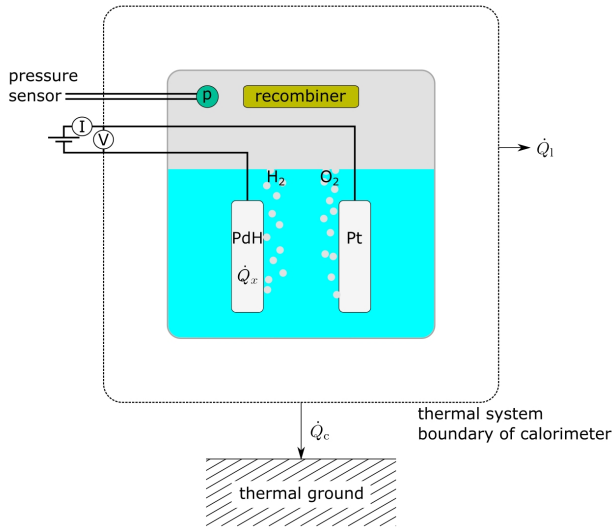

Fig. 2.2: Schematic illustration of a closed system calorimeter. $\dot{Q}_x$, heat sources or sinks to be identified, often referred to as *excess heat* in the literature; $\dot{Q}_c$, heat measured by the calorimeter; $\dot{Q}_l$, heat losses escaping measurement by the calorimeter; p, pressure sensor measuring pressure inside the vessel

2.5 Calorimetry Metrics

There are two metrics widely used in the LENR field:

1. Excess heat, $\dot{Q}_x$. In quasi-steady state (keeping input power constant), the excess heat is the difference between the output thermal power, P_{out}, and the input power, P_{in}:

$$\dot{Q}_x = P_{\text{out}} - P_{\text{in}} \tag{2.7}$$

2. Coefficient of performance, COP. In quasi-steady state, the COP is the output power normalized with the input power:

$$\text{COP} = \frac{P_{\text{out}}}{P_{\text{in}}} = 1 + \frac{\dot{Q}_x}{P_{\text{in}}} \tag{2.8}$$

A derived metric of the COP is the COP_e (with e for energy, as opposed to power). It is defined as the integrals of output power over input power:

$$\text{COP}_e(t) = \frac{\int_0^t P_{\text{out}} d\tau}{\int_0^t P_{\text{in}} d\tau}. \tag{2.9}$$

Due to limitations in experimental accuracies and varying sizes and input powers of electrochemical systems in the literature, COP has become a popular metric to normalize the excess heat with respect to the input power, even though it is not fundamentally clear why any processes generating excess power should scale with input power.

2.6 Sensitivity of Calorimetry

There are various mechanisms at play that limit the accuracy of a calorimeter:

- Accuracy of input power measurement: Ideally, all voltages and currents (electrochemistry, stimulation, heater etc.) must be measured at the thermal system boundary. In practice, this boundary might be poorly defined or it might be impractical to apply voltage sensors in that location.
- Faradaic efficiency variation: In open system calorimetry, the Faradaic efficiency might be less than unity, or generally change over time or with electrochemical current. In the absence of a flowmeter, this leads to inaccuracies in the accounting of chemical energy leaving the system. Even with flowmeters installed, it might be difficult to determine the chemical energy, given that the composition of the gas stream is unknown (e. g., some of the oxyhydrogen might recombine on exposed platinum).
- Recombiner inefficiency: There might be fluctuations in the reaction rates on the recombiner, depending on recombiner temperature, contamination with salt or liquid water. This leads to pressure buildup and a suppression of measured heat. Conversely, if oxyhydrogen has accumulated in the headspace and is being reacted by the recombiner, a transient increase in heat will be the result.
- Calorimeter efficiency: Even the best calorimeter will not capture all the heat put into the electrochemical system. Some of the heat will be transferred along poorly defined pathways, e. g., electric wires. These loss pathways might change over time, e. g., between calibration and experiment. Moreover, the thermal ground (environment) might change in temperature.
- Transient signals: In many experiments reported in the literature, the input power is varied over time. This leads to different steady state vessel temperatures depending on the input power (assuming a constant heat transfer resistance between the vessel and the thermal ground outside of the calorimeter). Depending on the thermal mass of the system and how the dynamics of the system are accounted for, this can lead to limited accuracy of the calorimeter for the duration of several thermal time constants after the input power change.
- Varying electrolyte level in open system calorimetry. Due to the nature of the open system and the ongoing electrolysis, the electrolyte level varies. This will likely change the heat transfer from the electrodes through the electrolyte into the vessel and the calorimeter.
- Calibration accuracy: Heat is not measured directly. Instead, typically a voltage is measured, representing a temperature (in an RTD) or a temperature difference (in a thermopile or thermocouple). Sometimes the conversion from temperature to heat is based on first principles (as in a thermal bar), but oftentimes it is based on calibration with a known input power (as in isoperibolic calorimeters). This input power might not be in the exact same location or have the same heat transfer resistance as the heat sources (electrodes, electrolyte, recombiner, lead wires etc.) during the experiment, leading to inaccuracies.

In addition to these fundamental limitations, which are present even in a well-behaved calorimeter, we have identified a variety of other potential causes for false signals; see section 9.2.

By performing calorimetry using various devices, we concluded that based on the fundamental limitations listed above, errors on the order of 1 to 10 mW in closed system calorimeters and several hundred mW in open system calorimeters are to be expected. The thermal time constant of common calorimeters is on the

order of tens of minutes, so any powers of interest exceeding those errors would have to be present for several minutes in order to be detectable. Postulating nuclear fusion events each with an energy of 24 MeV occurring over a period spanning the calorimeter time constant, a minimum of 10^{11} events (0.4 J) are required in closed calorimeters and 10^{14} events (0.4 kJ) are required in open calorimeters to be picked up by the calorimeter. For comparison, a Pd wire sample (25 mm length, 0.5 mm diameter) contains $3 \cdot 10^{20}$ atoms.

2.7 Calorimetry in the Literature

Various calorimeters have been described in the literature. Almost all LENR researchers built their own calorimeters, with the isoperibolic calorimeter being the most popular. It measures the temperature difference between a probe inside the vessel (in the electrolyte near the cathode) and a probe outside the vessel (which is held at constant temperature). Among others, McKubre [101], Energetics [102], Preparata [103], Letts [104] and Staker [105] used isoperibolic calorimeters. A major problem with this type of calorimeter is that the heat transfer resistance to the temperature probe in the electrolyte can change, e. g., due to bubbling depending on the electrolysis current or due to the presence or absence of a magnetic field [104, 106–109]. Moreover, submerging temperature probes into the highly alkaline, often warm, electrolyte for extended durations can result in their degradation, leading to faulty temperature readings. Most of the reported isoperibolic calorimeters were open. McKubre used a closed isoperibolic calorimeter as well mass flow calorimeters, where the heat is transfered to a liquid medium, the change in temperature of which is measured [110].

Groups involved with the Google effort created isoperibolic calorimeters that operate at elevated temperatures [93,111,112]. MacLeod et al. built a versatile calorimeter, not explicitly designed for electrochemistry, which can perform in-situ calorimetry on chemical reactions at up to 1232°C and 33 bar hydrogen pressure [111]. The sample is contained in a reaction tube, which is surrounded by a heater and an isothermal jacket. 14 thermocouples are placed in various locations and parameters of a heat flow model are fit to the thermocouple response during calibration. Young et al. built a miniature calorimeter around a solid state electrochemical cell with an RTD attached to the cell with an operating temperature of up to 1000°C [112]. Similarly to MacLeod, a model containing heat capacitances and resistors is fit to the readouts of the cell RTD as well as three other RTDs.

A more direct way to measure heat transfer across the thermal system boundary of the electrolysis vessel is to tile it with Seebeck sensors. These sensors are based on the thermoelectric effect, producing a voltage proportional to the temperature difference across the sensor. Examples of Seebeck calorimeters include those used by Storms [113] and Barham [106]. A related measurement method uses the Tian-Calvet principle, which covers the surface of the vessel of interest as well as the surface of a reference vessel with thermopiles [114]. Both vessels are contained in the same isothermal reservoir. (For a detailed description see section 2.8.1).

Most LENR studies neglect to account for the time-dependent response of the calorimeter when computing excess heat or COP. For example, when reducing the input power (e. g., stepwise), an apparent excess heat (as defined in eq. 2.7) is to be expected for a few thermal time constants of the calorimeter until it has sufficiently approached its new steady state. To address this problem, McKubre and Storms used compensation heaters to keep the total input power constant [110,113]. In the absence of such a heater, the electrolysis input power should be kept constant, or the metrics of excess heat and COP will result in erroneous readings as the system adjusts to its new steady state upon a change of input power. Notably, Chiang et al. characterized the instrument response function in order to model the dynamic system behavior and thus enable interpretation of excess heat and COP across input power changes [115]. (For further reading, see section 2.9.1.)

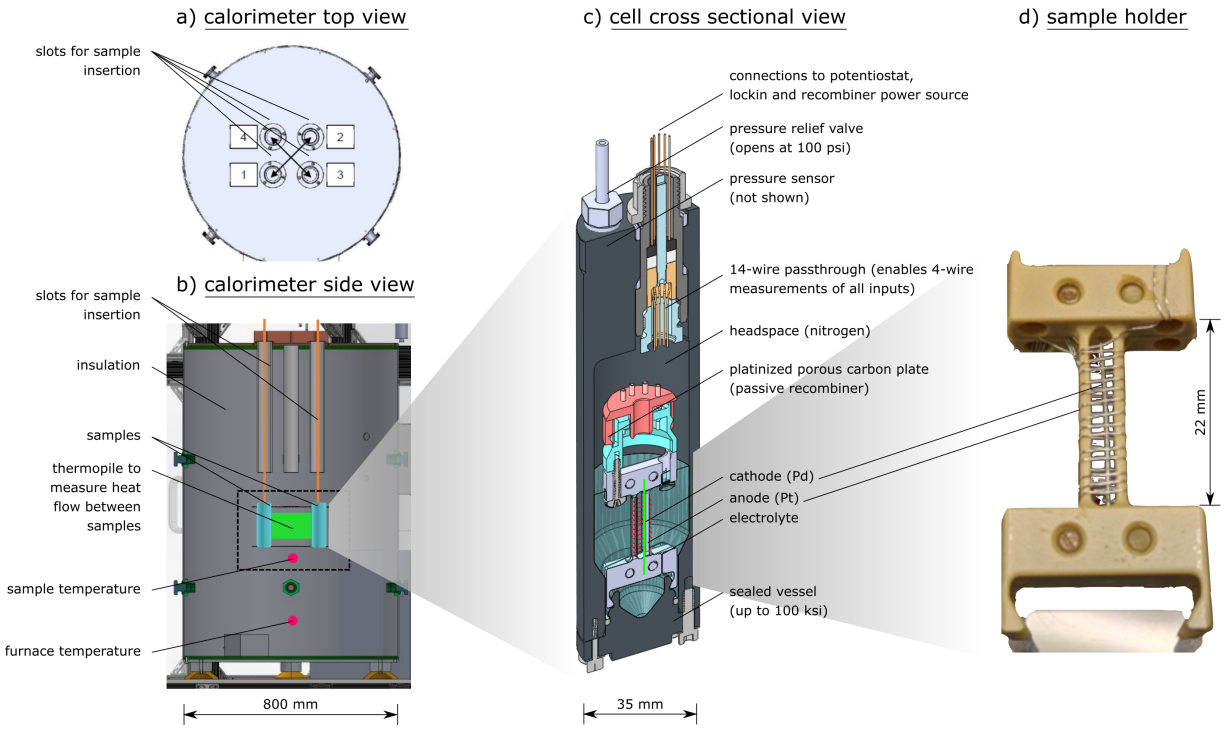

Fig. 2.3: Setaram MS80 calorimeter setup. a) Calorimeter top view, showing the relative heat measurements between cells 1 and 2, and cells 3 and 4. b) Calorimeter side view, showing the location of the in-situ cells within the calorimeter. c) Cell cross-sectional view, showing all major components of the electrolytic cells (custom made). d) Photograph of the sample holder made from PEEK polymer, showing the electrode arrangement.

2.8 Setaram MS80

2.8.1 Hardware

The Setaram MS80 is one of the most accurate commercially available calorimeters with a sample space large enough to accommodate a custom-made apparatus for in-situ calorimetry during electrochemical experiments (Fig. 2.3). It is based on the Tian-Calvet principle. It contains four bores for samples, each of which is surrounded by a thermopile measuring the heat flow between the bore and an isothermal block. The four thermopiles are configured as two pairs of sample and reference cells. For each pair, the differential heat flow between the sample bore and the reference bore is measured. Each bore has an inner diameter of 35 mm and a depth of 500 mm, of which the lower 100 mm is covered with thermopiles.

We designed and built vessels for closed system electrolysis experiments that fit into the MS80 bores (Fig. 2.3 c). Each vessel contains a palladium cathode (typically a 0.5 mm diameter, 25 mm length wire, though various sample geometries can be accommodated), a helically wrapped platinum anode (0.2 mm diameter) with an electrode spacing of ~ 3 mm, a recombiner (platinized carbon plate, fuelcellstore.com, SKU 72500511,

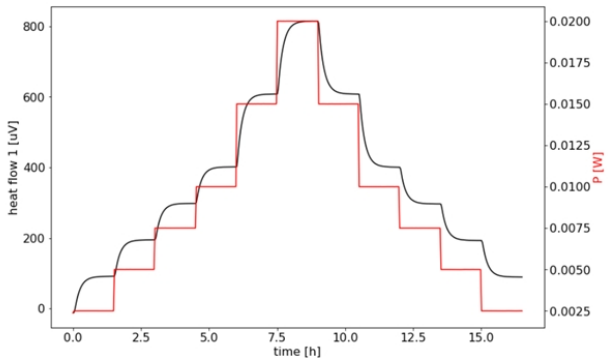

Fig. 2.4: Calibration of MS80, using a staircase of known input powers into the calibration resistor to obtain a conversion factor from reported thermopile voltage (called 'heat flow 1 [uV]' in the MS80 software) to heat flow. Calibration resistor input power is plotted on the right axis, shown as the red curve. The resulting thermopile voltage is plotted on the left axis, shown as the black curve.

65 mm x 8 mm), a calibration resistor (for resistive heating during calibration) and a pressure transducer. The vessel is filled with 17.7 ml electrolyte, leaving a headspace of ~ 23 ml. A pressure relief valve at the top of the vessel opens if the vessel pressure exceeds 7 bar. Because detonations could result in pressure transients faster than the reaction time of the relief valve, the vessel is designed to withstand pressures of up to 700 bar. The sample resistance is continuously measured using a four-wire measurement, with the lead wires (0.13 mm diameter Pt wire coated with PFA, A-M Systems) laser-welded onto the sample wire. The spacing between the current supply leads is ~18 mm and the spacing between the voltage sense leads is ~12 mm. The lead wires for the electrochemistry, the resistance measurements (to determine loading) as well as for optional axial electromigration currents along the cathode are routed through a custom-made feedthrough at the top of the vessel. The voltage sense locations for all electrical power inputs into the vessel are located just outside of the vessel. The currents for electrochemistry and axial currents are provided by computer-controlled current sources (BioLogic VSP 300, Keithley, NI-PXIe 4141, NI-PXIe 4144, NI-PXIe 4145, NI-PXIe 4154, depending on use case). The voltages are measured using either the four-wire probe provided by the current source instrument or are independently measured using a voltmeter (Keysight 34461A or NI PXI-4071, NI PXI-4081).

2.8.2 Calibration

The heat flow is measured using the software provided with the MS80. In order to convert the reported differential thermopile voltage to a heat flow, we perform a calibration, inputting a known power into a calibration resistor mounted within the electrolyte close to the electrodes (Fig. 2.4). A linear fit to the steady state relationship between input power and thermopile voltage yields a conversion factor to compute the heat flow based on the reported voltage. The reference (control) cell is typically a vessel with a comparable configuration and similar input powers, however either both electrodes are platinum or the electrolyte is light water, to act as a control. The input power is taken as the sum of all electric input powers (electrochemistry, axial current, resistance measurement, resistor calibration), with the voltage senses near the thermal system boundary of the calorimeter. Excess heat and COP were computed following equations 2.7 and 2.8. The

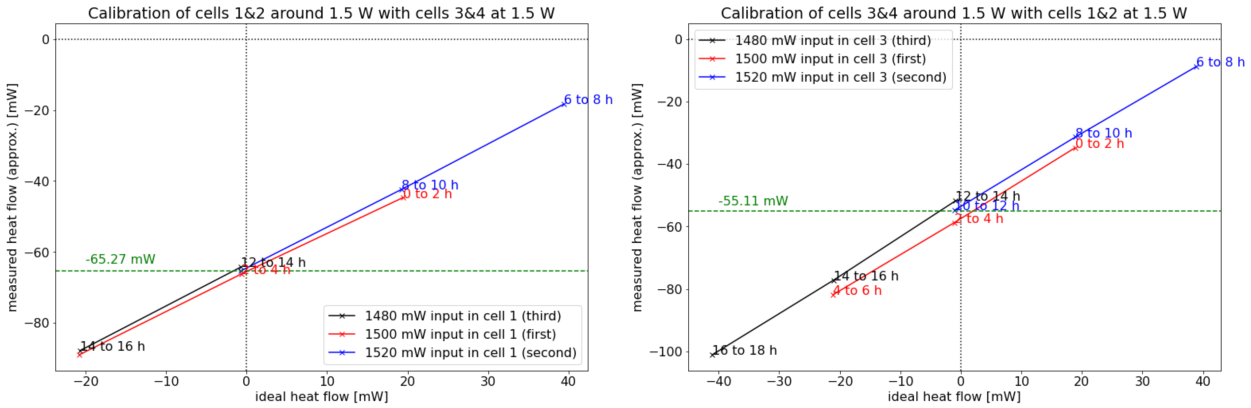

Fig. 2.5: Calibration of MS80 with 1.5 W input power in the reference cells (cells 2, 4) and 1.5 W ± 20 mW in the experiment cells (cells 1, 3), showing an offset of ~ 60 mW between the measured heat flow and the input power (~ 4 %).

MS80 accuracy specification covers differential and absolute heat flows up to 500 mW. However, we often operated at input powers of up to 3 W for both vessels in a pair, with differential heat flow up to 500 mW.

In order to ensure accurate measurements while operating outside of the specified range, we performed calibrations with known input powers in the experiment cells and the reference cells. For instance, Fig. 2.5 shows how there was an offset of ~60 mW between the measured heat flow and the input power (~ 4 %).

In addition, there is some sensitivity to the type and location of the heat source. As shown in Fig. 2.6, if both cells' input power is applied through electrochemistry, the indicated heat flow from cell 2 to cell 1 is 50 mW at 1.5 W input power (a 3 % false signal). If a calibration resistor (placed within the electrolyte near the electrodes) is used instead of the electrochemistry, a false heat flow signal of up to 150 mW (10 %) is measured. In the extreme case, when the heat originates from a resistor in the headspace in the reference cell (cell 2), a heat flow of 300 mW (at 1.5 W electrochemical input power in the experiment cell 1) is measured, corresponding to a false heat flow signal of up to 20 %. This is likely due to the different coupling of heat sources to the thermopile and to the loss pathways (wires leading to the vessel, top and bottom faces of the vessel).

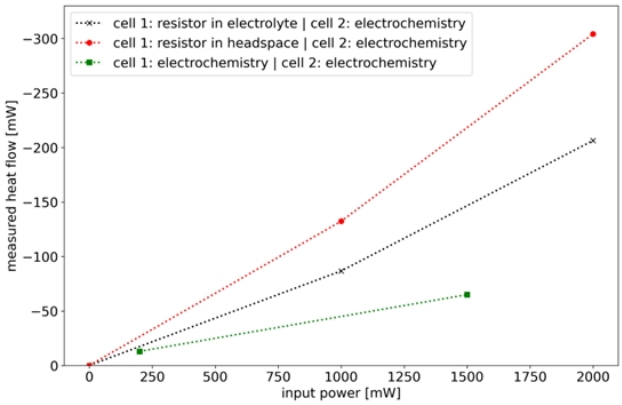

Fig. 2.6: Location dependence of power input in MS80 calorimeter leading to false differential heat signals despite equal power inputs. The sign convention is that positive heat flow is from cell 1 to cell 2.

2.9 High-throughput Calorimeter (HTcal)

As an alternative to the bulky and expensive Setaram MS80 with its industry-leading accuracy, we employed various homemade calorimeters, which were designed for ease of use, enabling a higher sample throughput to cover a large parameter space in a short amount of time. We noticed that the heat flow accuracy of the MS80 was limited by the fluctuation in recombiner efficiency rather than the calorimeter itself, so we could not take full advantage of the MS80's capabilities in any case.

2.9.1 Design Objectives

We dubbed this type of high throughput calorimeter the *HTcal*. Its distinguishing features are:

- Closed system calorimetry: To reduce the number of potential false signals, closed system calorimetry is essential. Pressure is monitored in order to diagnose recombination events (which represent the most frequent cause for false elevated COPs).
- Single-ended calorimetry: As opposed to the MS80, the HTcal measures heat flow against a thermal ground as opposed to against a reference cell. This design allows us to accommodate twice the number of experimental vessels in a given space and eliminates the time to set up reference cells.
- Direct measurement of heat flow: Using a thermal bar (Fig. 2.7a) of known geometry and known thermal conductivity, we convert the measured temperature gradient to heat flow (eq. 2.10). This design makes fewer assumptions than other designs relying heavily on calibration (e. g., isoperibolic calorimeters with a single temperature sensor). Linearity of the temperature along the thermal bar verifies accuracy. Five sensors ensure reliable measurements even if one or two sensors are faulty.
- Streamlined sample mount: The sample is clamped between platinum contacts. This is much easier than laser welding and proved to form a reliable electrical connection even after multiple load-deload cycles. Four contacts are provided to enable a four-wire resistance measurement to determine the loading.

- Streamlined vessel assembly: The vessel is operated at pressures up to 6 bar, with a burst pressure of 15 bar. The moderate burst pressure enables the usage of a PEEK lid, containing all passthroughs. Electrical passthroughs are made with commercially available connectors (LEMO) and gas connections for the vent line and the safety relief valve are made with push-to-connect fittings.
- Streamlined architecture: Almost all electrical devices, such as current sources (EC, EM, calibration) and measurement devices, e. g., multimeters (DMM) and temperature sensors (RTDs) for environmental monitoring and heat flow calculation, are unified into a NI PXI system (Fig. 2.7c).
- Streamlined data recording and analysis: All data streams are recorded using Python in Jupyter notebooks and saved into a database. Analysis is done in Python as well.

2.9.2 Operating Principle and Implementation

Fig. 2.7 b shows a photograph of the HTcal. It typically contains four electrolytic cells sharing a thermal baseplate. The centerpiece of each cell is a vessel (made from aluminum, lined with a 0.5 mm thin machined PEEK liner) which is connected through a thermal bar to a thermal ground (an isothermal aluminum base plate, the temperature of which is controlled through a Peltier element, TE Technology CP-031). About 90 % of the heat generated inside the vessel leaves through the thermal bar, while the rest escapes through less well-defined pathways (e. g., through the insulating closed-cell foam or along the electrical or gas lines).

The measurement principle is to measure the temperature gradient along the thermal bar. It is related to the heat flow $\dot{Q}$ as follows:

$$\dot{Q} = kA\frac{dT}{dx} \tag{2.10}$$

with k being the thermal conductivity of the thermal bar, A being the cross sectional area of the thermal bar and $\frac{dT}{dx}$ being the temperature gradient along the thermal bar. For a robust determination of the gradient, we measure the temperature in five locations along the thermal bar. The spacing between locations is 10 mm. This determines the length of the thermal bar (65 mm). The diameter of 17 mm is determined by the optimum balance between maximizing the sensitivity (smaller diameter results in larger temperature gradient at a given heat flow) and minimizing the thermal time constant (larger diameter results in shorter thermal time constant) to resolve transient signals. The Peltier element keeps the base plate at a constant temperature (typically 30°C) with a standard deviation < 10 mK. The enclosure temperature is kept constant with a standard deviation of 30 mK by using two stages (preconditioning chamber, calorimetry chamber) of heater fans conditioning the air from the lab. The fans run continuously, while the heaters (Stego 03114.9-00 HVL031 DIN Rail Enclosure Fan Heater 300 W 120 VAC) are controlled by a PID thermostat with a continuous output (made in house). The temperature uniformity within the thermal enclosure is ensured by a large mixing fan.

2.9.3 Calibration and Performance

Figure 2.8 characterizes the performance of the HTcal. A typical calibration procedure for a four-cell unit is shown in Fig. 2.8a, with resistor input powers up to 2 W. A selection of resulting temperature profiles along the thermal bars is shown in Fig. 2.8b. *Corrected temperature* refers to the correction to compensate for RTD offsets, as Pt100 RTDs typically yield readings with sensor-to-sensor variations of ~0.2 K when all the sensors are attached to the same thermal ground. The temperature gradient is obtained through a linear fit to the temperature profiles, resulting in the measured heat flow (using eq. 2.10, Fig. 2.8c). The measured

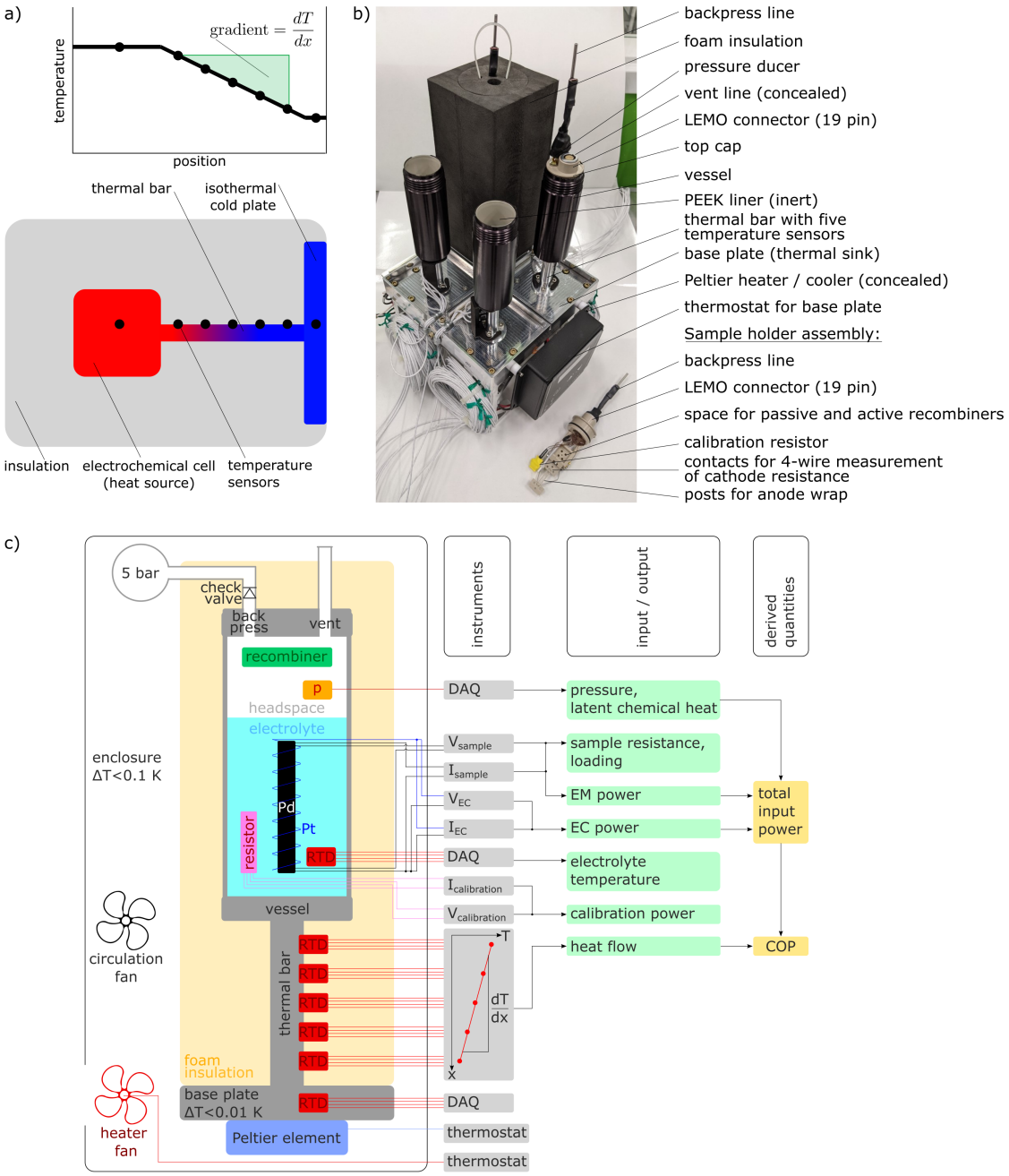

Fig. 2.7: High-throughput calorimeter (HTcal). a) Heat flow measurement principle of thermal bar (see eq. 2.10). b) Photograph of an HTcal unit with four cells. c) Electrical diagram of HTcal. Note that the vent port is closed during experiments.

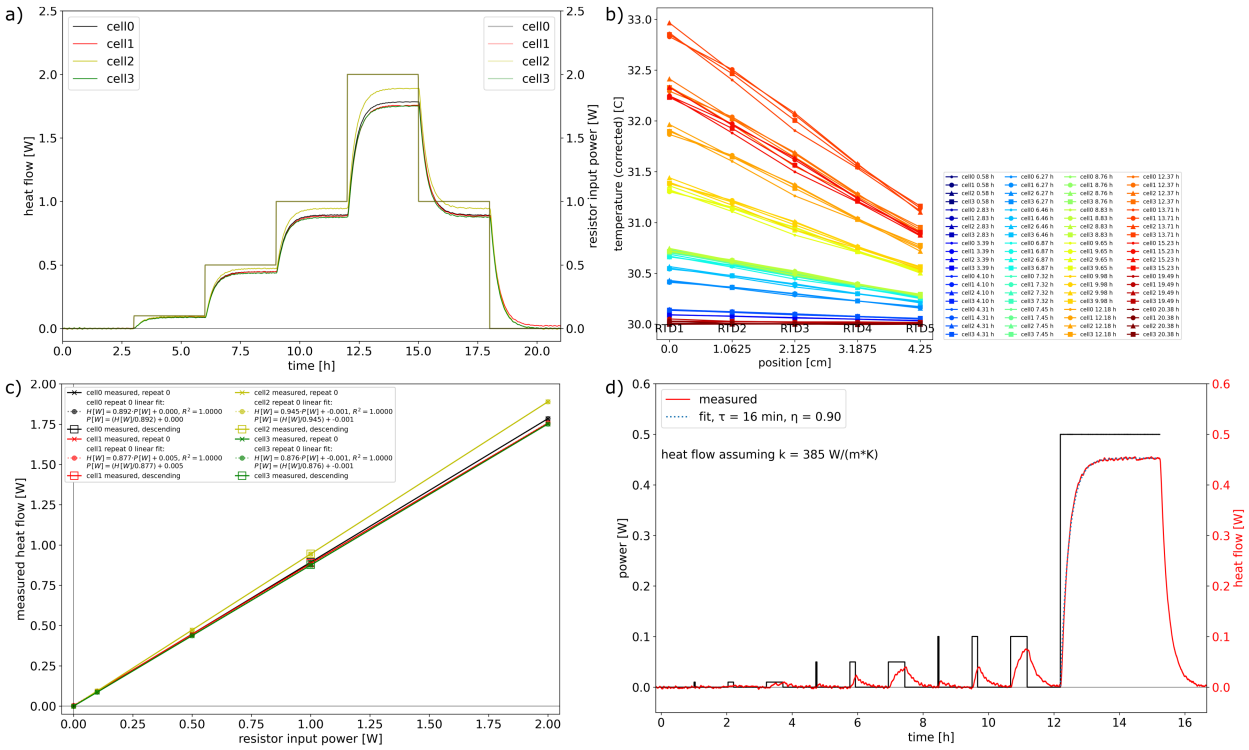

Fig. 2.8: HTcal calibration. a) Staircase calibration procedure to investigate linearity of measured heat flow vs. calibration resistor input power. b) Temperature profiles along thermal bar during application of staircase calibration. c) Measured heat flow from temperature profiles vs. calibration resistor input power, along with linear fits. The open symbols refer to the descending step, showing that there is no significant drift or hysteresis. d) Application of calibration resistor input power pulses of [2, 10, 30] minutes length and [10, 50, 100] mW power with a final 3-hour, 500 mW step, along with simple exponential fit of $\tau = 16$ min and an efficiency of $\eta = 0.90$.

heat flow varies linearly ($R^2 = 1.0000$) with the calibration resistor input power, with a constant of 0.89±0.05 (the calorimeter efficiency, η). In other words, about 90 % of heat put into the vessel leaves through the thermal bar. As mentioned previously, the efficiency is a trade-off between sensitivity and time resolution. Depending on the thermal bar geometry, the thermal time constant of the HTcal is around 15 to 25 minutes (Figs. 2.8d and 2.14a). This allows us to resolve a 30-minute 10-mW pulse or a 2-minute 50-mW pulse. η is a function of the vessel and thermal bar and varies typically $< 0.5\%$ when repeating a calibration for a given assembly and $< 2\%$ when repeating a calibration before and after assembling a cell.

2.9.4 Excess Heat Metrics during Transients

Previously, we introduced excess heat $\dot{Q}_x$ and COP (eqs. 2.7 and 2.8). While these equations hold true in principle (and are a good approximation in steady state), the measured heat flow not only depends on

the power leaving the vessel, P_{out}, but it is also a function of the calorimeter, in particular its instrument response function F. As can be seen in Fig. 2.9a) and b), after application of a step function to the input power, the expected heat flow (assuming $\dot{Q}_x = 0\,W$) approaches steady state gradually, in theory following the convolution of the input power P_{in} with the impulse response function F:

$$\dot{Q}_{\text{expected}} = P_{\text{in}} \circ F \tag{2.11}$$

In practice, we obtain the impulse response function F as the derivative of the measured heat flow after an input power step (Fig. 2.9a). Often, the impulse response function is represented by an exponential fit, but we found that using an empirical response function gave better results. Using the quantity of *expected heat flow*, we can define the excess heat and COP, accounting for the calorimeter response:

$$\dot{Q}_{x,\text{convolved}} = \dot{Q}_{\text{measured}} - \dot{Q}_{\text{expected}} \tag{2.12}$$

$$\text{COP}_{\text{convolved}} = \frac{\dot{Q}_{\text{measured}}}{\dot{Q}_{\text{expected}}} \tag{2.13}$$

with $\dot{Q}_{x,\text{convolved}}$ being the excess heat (convolved) and $\text{COP}_{\text{convolved}}$ being the COP (convolved). Figs. 2.9c) and d) illustrate that generally $|\dot{Q}_{x,\text{convolved}}| << |\dot{Q}_x|$ and $|\text{COP}_{\text{convolved}} - 1| << |\text{COP} - 1|$, in particular after input power changes.

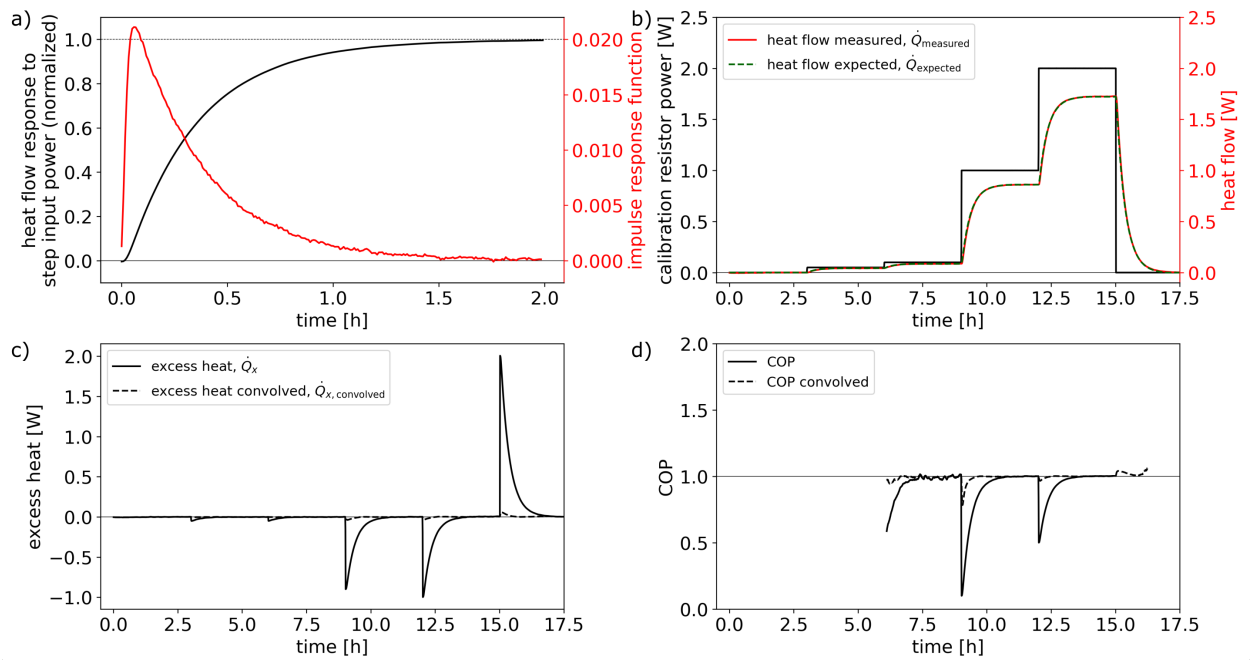

Fig. 2.9: Accounting for transient input powers in HTcal. a) Heat flow response to step input power (normalized, step at time = 0 h) along with impulse response function (derivative of heat flow response). b) to d) Application of impulse response function convolution to a calibration experiment. b) Calibration resistor input power follows a staircase. The expected heat flow, computed using eq. 2.11 closely fits the measured heat flow. c) The excess heat, $\dot{Q}_x$ shows major depressions following input power increases, owing to the thermal mass of the system. After accounting for it, the excess heat (convolved), $\dot{Q}_{x,\mathrm{convolved}}$ is much closer to 0 W after input power changes. d) COP (convolved) is much closer to unity than COP.

2.10 Ultra-high Throughput Calorimeter

2.10.1 Introduction

To date, electrochemical experiments run for the purpose of creating and detecting Anomalous Heat Events (AHE) have been primarily run in our High Throughput Calorimeters (HTcal). Hundreds of experiments have been run over the years, typically using clusters each consisting of four calorimeters (section 2.9.1) and running for days to weeks. Many lessons have been learned, but no definitive signs of AHE were found. A potential explanation could be that there is only a small statistical likelihood in which AHE will occur. To explore this space, more calorimeters running for longer durations would be required. Replicating the HTcal systems to increase experimental throughput is expensive from both budget and real estate points of view. To address these issues, an Ultrahigh Throughput Calorimeter (UHTP) system was developed. This system consists of 100 electrochemical cells with in-situ calorimetry running in parallel for an indefinite length of time (Fig. 2.10). The UHTP program increased our experimental throughput by nearly 5x, going from 26 to 126 calorimeters. The purpose is to screen vast parameter spaces and to detect excess heat signals of at least 100 mW (typically COP > 1.2). If we find signals of that magnitude, we can investigate those samples more closely in the MS80 or HTcal.

The UHTP system was designed with cost and scalability in mind. A custom PCB was developed to consolidate the required functions of the general-purpose National Instruments PXI chassis onto a single board (Fig. 2.11). Power and data was provided via Power over Ethernet (PoE), reducing system cable count. Experimental control, data transfer and storage are handled by Python running in a Jupyter notebook on a general purpose computer. Data is then replicated on our internal servers for analysis. The electrochemical vessel is borrowed in part from the HTcal design. It has been updated to be mass-produced by a contract manufacturer.

The UHTP PCB can supply up to 10 W (10 V at 1 A) of electrochemical power and drive up to 4 A of electromigration current into a milliohm load. The electromigration current is additionally used to measure the resistance of the sample with a resolution of 100 µΩ. Integrating power meters on both the electrochemical and electromigration power supplies can measure electrical input power to the cell with 1 mW accuracy. RTDs located in the electrolyte and on the base plate measure temperatures with 100 mK accuracy. A pressure transducer measures the pressure in the vessel with a resolution of 24 µpsi and a temperature accuracy of 100 mK.

2.10.2 System Architecture

2.10.2.1 Overview

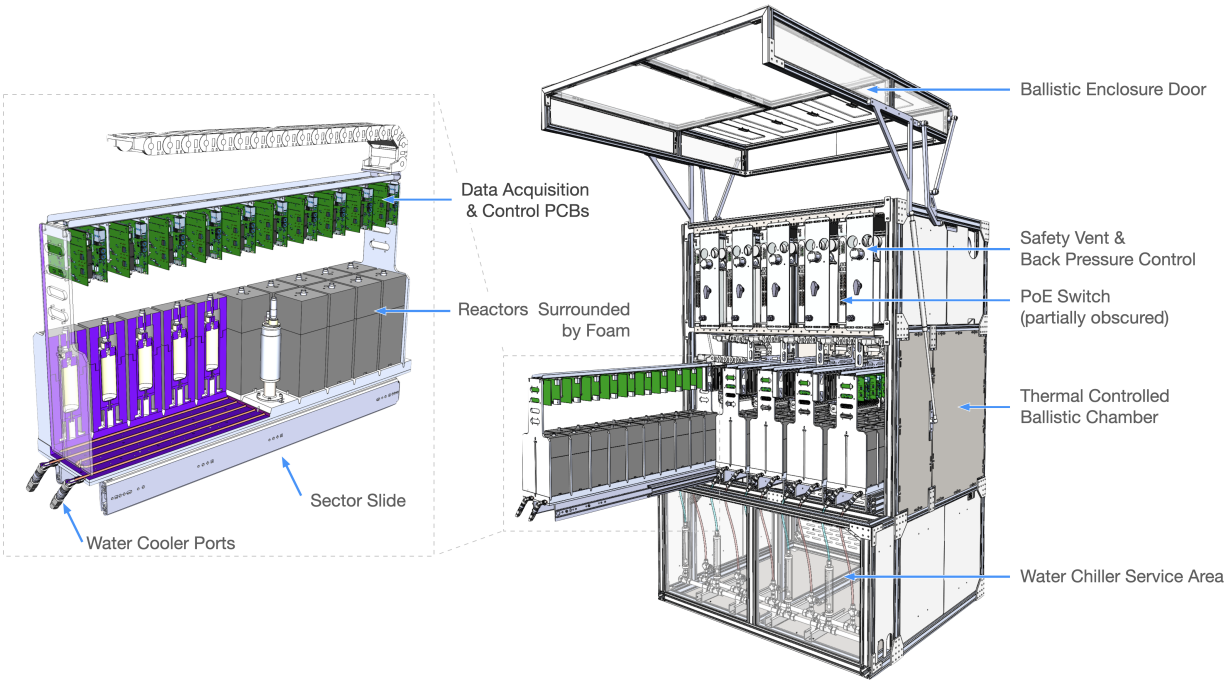

Fig. 2.10: UHTP enclosure with detailed sector breakout.

The UHTP system consists of the following main components (Fig. 2.10):

1. Super Structure: The Super Structure functions as both the primary structural framework and a protective safety barrier for the UHTP system. It contains Ethernet switches for communication, thermal enclosure and over pressure relief infrastructure for the calorimeters.
2. Reactors: 100 closed isoperibolic electrochemical calorimeters containing a variety of electrochemical cells.
3. Thermal Enclosure: Provides a constant temperature enclosure used to minimize parasitic reactor heat exchange with the environment.
4. Sectors: Each sector contains 20 calorimeters, their supporting PCBs, and a water cooled base plate.
5. Power System: To minimize cable count in the system, Power over Ethernet (PoE) is used for both power and data transfer.
6. Reactor Control and Data Pipeline: A system to send commands to and receive data from the reactors (Fig. 2.11).

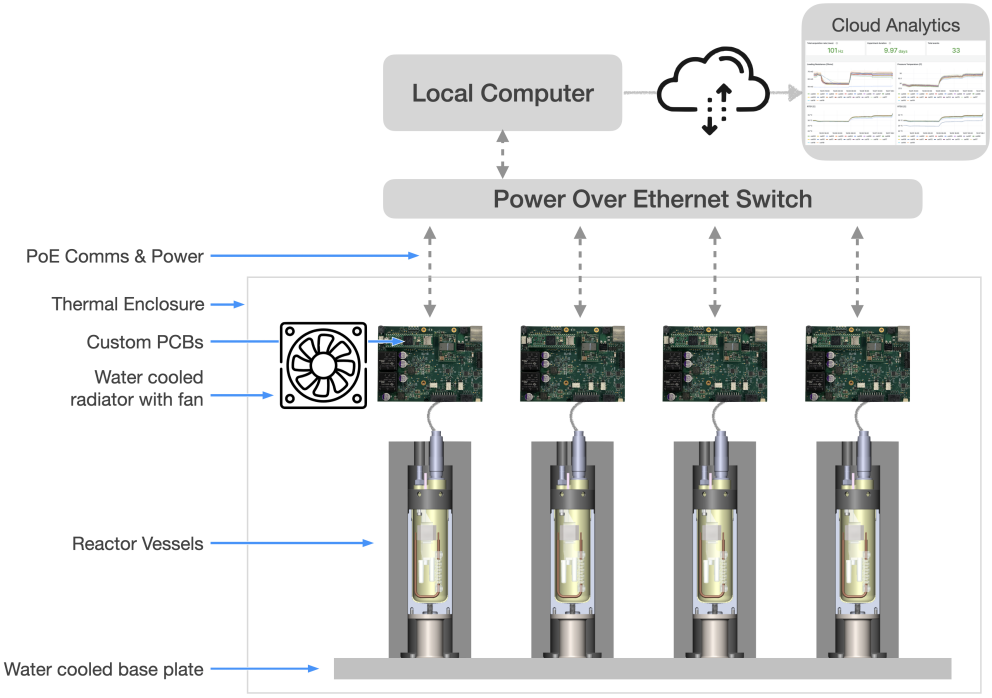

Fig. 2.11: System Diagram

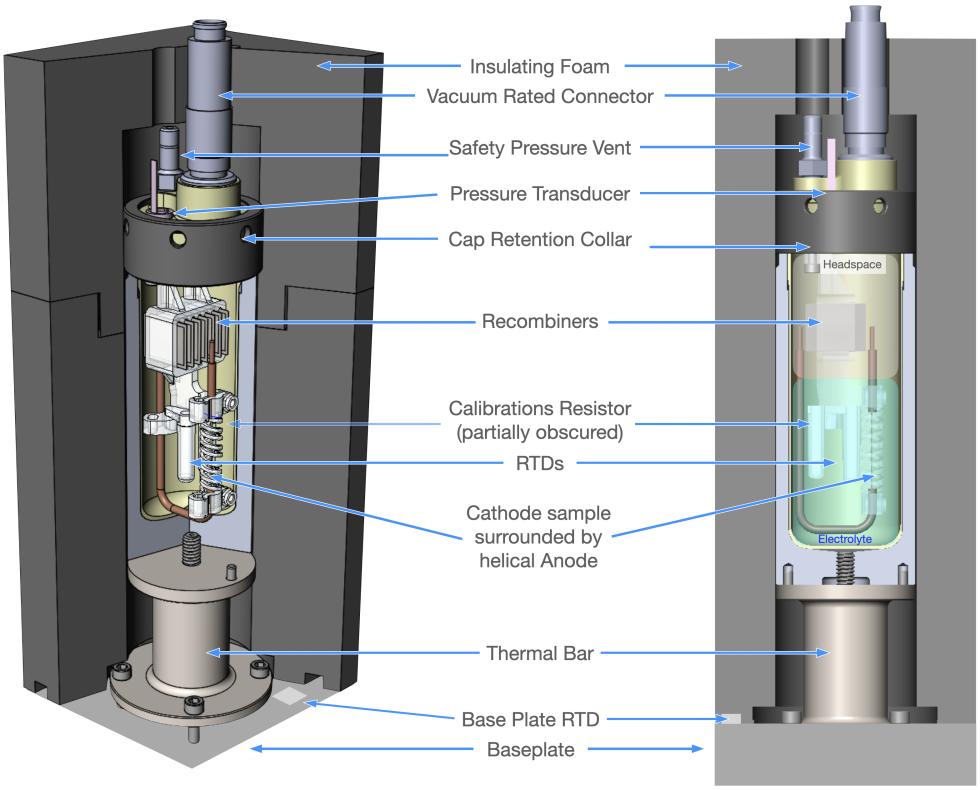

Fig. 2.12: Schematic cross-sectional views of a UHTP vessel.

2.10.2.2 Reactors

The UHTP reactor is a closed isoperibolic calorimeter largely based on the HTcal design with a few modifications (Fig. 2.12). Heat flow is calculated from the temperature difference between the electrolyte temperature and the base plate temperature, based on calibrations with known input powers. Constant base plate temperature is achieved by using water cooled base plates to remove nearly all heat from the cells. Water cooled radiators and fans are used to remove heat generated by the PCBs and to ensure uniform air temperatures throughout the enclosure. This reduces the amount of heat added or removed from the cells by ambient air. RTDs are prone to failure over time due to the corrosiveness of the electrolyte. Unlike HTcal, which measures heat flow using an external thermal bar, UHTP relies solely on the temperature difference between the electrolyte and base plate. A second RTD was added to mitigate a single point of failure. Switching heat flow measurement methods from a thermal gradient to a ΔT reduced the sensitivity of the system. To compensate for this, the thermal bar was altered to increase its thermal impedance and therefore sensitivity to ensure small signals would not go undetected.

Each reactor contains a cathode (typically a 25 mm long by 0.5 mm diameter wire sample) of either palladium (active cells) or platinum (control cells). The cathode is surrounded by an anode consisting of

230 mm long 0.2 mm diameter platinum wire completing approximately 12 revolutions at a radius of 3 mm. The electrodes are submersed in 48 ml of either LiOD (active cells) or LiOH (control cells). In a typical experiment, each sector contains 17 active and three control cells totaling 85 active and 15 control cells for the UHTP system.

Each reactor is surrounded by thermal foam, designed to direct the majority of heat flow from the reactor through the thermal bar and into the base plate, thereby minimizing heat exchange with the surrounding environment.

2.10.2.3 Thermal Enclosure

As mentioned in the reactor section, the primary heat transfer pathway in the system is from the reactor to the base plate. However, several additional routes exist for heat to enter and exit the reactor. To minimize heat exchanged with the environment, an insulated thermal enclosure is employed. The thermal enclosure uses water-cooled radiators and fans to assist the base plate in maintaining a constant temperature outside of the reactors.

An effort was made to keep all heat sources (PoE switches, circulation fan power supplies, water pumps, etc.) outside the thermal enclosure to minimize the exchange of parasitic heat with the reactors. Due to high electromigration current (3 A) an exception was made for the control and data acquisition PCBs. A comprehensive trade-off analysis led us to prioritize signal integrity between cells and PCBs, as well as ease of assembly and servicing, over optimal thermal performance. Although placing components outside the enclosure would enhance thermal management, the chosen configuration offers a better balance of overall system efficiency and practicality.

2.10.2.4 Sectors

Bringing 100 reactors online at once in a new system can be risky. Physically working with a large number of reactors is also challenging. To keep UHTP easy to work with and scalable, 100 reactors were designed to be built in sectors of 20 cells each as shown in Figure 2.10. The calorimeters are arranged in a two wide by 10 deep configuration. When the enclosure is fully populated, it contains a ten by ten array of 100 calorimeters. The sectors are built on slides allowing for easy access and quick installation of calorimeters. As designed, the UHTP enclosure can run with one to five sectors installed. Each sector has its own PoE switch and chiller attachment points. This allows the system to be built up, repaired, or upgraded in sections. This also enables parallel workflows as the system can be run while work takes place on sectors outside the enclosure.

2.10.2.5 Power System

Power over Ethernet (PoE) is used to power the PCBs. The PCBs have isolated power supplies that convert 48 V PoE voltage to the 0-10 V required for electrochemistry and 100 mV at 4 A required for electromigration and sample resistance measurements. This system is designed to carry out long duration experiments (~ two months). In the event of a mains power failure, the entire system is backed up with an Uninterruptible Power Supply (UPS) that can maintain full system operation for 3-4 hours.

2.10.2.6 Reactor Control and Data Pipeline

At the center of the UHTP Reactor Control and Data Pipeline is a general purpose computer. This computer sends control commands and receives data from the micro-controller on the PCBs via Ethernet using

JavaScript Object Notation (JSON). JSON was chosen because it is a lightweight and human readable protocol, easy to implement and debug. This computer stores the data in a local database as well as replicating it to the cloud based Science Hub database where it's further processed using Python with the Pandas package.

Each PCB has a unique IP address that is manually configured using rotary hexadecimal switches on the board. This method allows us to easily encode the reactor's physical location in the array into the last two octets of the IP address. Knowing the cell locations relative to each other is key in understanding potential thermal crosstalk between the cells. It also helps identify potential gradients in a uniform temperature enclosure. In this experiment, the reactors are arranged in a 10 x 10 array. For instance, IP address 192.168.1.2 refers to the reactor in the second column and in the third row (with counting starting at 0).

In addition to controlling the vessels, the custom PCBs monitor environmental conditions such as enclosure temperature, pressure release rail pressure, room temperature, and barometric pressure.

2.10.3 Safety

There are several factors that could potentially cause hazardous conditions and/or events. The UHTP enclosure was designed to mitigate three main hazards.

1. Pressure buildup: Electrolysis produces heat and oxyhydrogen which pressurizes the cell. If this is not addressed, the cell could potentially explode due to over pressure or rapid recombination. To mitigate this, recombiners are employed to recombine oxyhydrogen into water in a controlled manner. In addition to recombiners, there is a safety relief valve that will vent the cell if pressure exceeds 85 psi.

2. Runaway AHE: Should a larger than anticipated AHE event occur, it is possible this could cause the cell to explode. To mitigate this as well as events where the recombiners and safety vent fail, the cells are located in a ballistic enclosure designed to contain shrapnel in an explosive event.

3. Oxyhydrogen builds up in the enclosure: If the safety vent system or the cells leak, oxyhydrogen may enter the enclosure itself. This gas can accumulate and create a hazardous condition. To mitigate this, a fan cycles room air through the enclosure and exhausts it into the laboratory exhaust vent. This is done at a rate such that the enclosure volume is replaced every 36 hours.

Reactors are controlled en masse from one to several notebooks. Should a safety event occur that affects one or more reactors, a command can be issued to shut down or restart reactors individually without affecting other reactors in the same controlling notebook.

2.10.4 Measuring Performance

The goal of this effort is to produce more energy than is consumed. There are two metrics used to measure performance: Coefficient of Performance (COP) and excess heat flow (see section 2.5).

Accounting for measurement system error, the excess heat calculation is a reliable metric for determining if a cell is producing more power than it is consuming. What this metric does not tell is the efficiency of the system. It is important to know if it took 1 W or 1 kW to produce 100 mW of excess heat, which is captured in the COP.

At a minimum, both COP and excess heat should be used to determine if the system is in fact producing excess heat.

2.10.4.1 Calibration

To calculate COP and excess heat we must know input and output power. Input power is easily and accurately measured and in the form $P_{\text{in}} = VI$, with I being the current and V being the voltage (for each electric circuit entering the calorimeter). The voltage is measured close to the thermal system boundary.

Measuring output power is not as straight forward. Unlike HTcal, where output power is measured via a temperature gradient across a thermal bar, heat flow in UHTP must be inferred by measuring the electrolyte to base plate temperature difference, ΔT, and knowing the thermal impedance of the system, Z_{th}.

$$P_{\text{out}} = \frac{\Delta T}{Z_{\text{th}}}$$

Z_{th} is found empirically by calibration. There are several sources of heat in the UHTP system. Heat due to ohmic heating of the electrolyte (from electrochemical current), heat due to (electro-)chemical reactions (at the electrodes and at the recombiners), heat due to the electromigration current passing through the cathode and the lead wires, and hopefully excess heat from low energy nuclear reactions. Each source of heat takes a slightly different path from source to the base plate. The Z_{EC} path, resulting from application of electrochemical voltage to the electrodes, is dominated by electrolyte. Given that the electrolyte resistance is much greater than that of the wires, relatively little heat is lost in the wires. As such, heat due to electrochemistry is tightly coupled from the electrolyte to the vessel wall to the thermal bar.

Unlike the electrochemistry electrical circuit, the electromigration electrical circuit is essentially a loop of wire with two thirds of this loop residing outside of the immediate electrolytic cell. The voltage sense lines of the electromigration power meter were attached immediately outside the reactor. This is to ensure heat dissipated into the reactor is accounted for while the parasitic heat from the wire harness is not. Also, unlike the electrochemistry thermal path, which is from the electrodes to the electrolyte and to the vessel walls, only about half of the electromigration power is coupled into the electrolyte. The rest is coupled to the vessel via the head space and wires leading to the PCB. This is the reasoning for using separate thermal impedances for electrochemistry and electromigration.

Determining the thermal impedance of unknown heat sources, Z_x, is a challenge as we would need to know the location of the unknown heat source and how it couples to the temperature sensors in the electrolyte. For now we can assume Z_x is bounded by Z_{EC} and Z_{EM}. For the purposes of this paper and the UHTP experiments, a Z_x value of 5.5 K/W is assumed. If Z_x is in fact bounded by Z_{EC} (5.8 K/W max) and Z_{EM} (4.1 K/W min), this would yield a maximum error of 22 %.

Determining Z_{EC} is done by applying a constant power to the power resistor that resides in the electrolyte. While any amount of power can be used for calibrating the reactor, once the relationship between power input and change in electrolyte temperature was demonstrated to be linear, 2.5 W was chosen for calibration, as it is the average of the power levels intended to be used in the system. The resistor is used as a proxy in lieu of an electrochemical heat source. We verified that the calibration with resistors closely matches the calibration with inert electrodes.

Z_{EM} is found by applying 3 A DC to the cathode. This results in ~600 mW being sourced into the system with ~300 mW of heat being dissipated in the electrolyte.

Calibration begins after the enclosure has dwelled for 24 hours to ensure it has equilibrated. EC calibration begins by applying 2.5 W to the power resistor and letting the electrolyte temperature reach equilibrium after five time constants of 43 minutes each. Power is removed and the calorimeters are allowed to dwell for five time constants to return to equilibrium. A current of 3 A is then applied to the cathode for five time constants. Power is then removed, and the enclosure is allowed equilibrate for five time constants before the

experiment begins. It should be noted that power into the cell, electrolyte, and base plate temperature are recorded at a 1 Hz rate during calibration.

To investigate the linearity of the calorimeter, a staircase calibration was performed at 150 mW, 250 mW, 500 mW, 1 W, and 2.5 W resistor powers (held for several thermal time constants, Fig. 2.13). After validating that the thermal impedance is independent of the resistor input power, calibrations were performed at a single power level.

Along with the steady state thermal resistance, the instrument response functions, S_{EC} and S_{EM} are obtained during calibrations. This enables us to calculate the expected electrolyte temperature during the transients in EC power and EM power. The expected temperature difference (between electrolyte and base plate) is calculated as follows:

$$\Delta T_{\mathrm{expected}} = (P_{\mathrm{EC}} Z_{\mathrm{EC}}) \circ S_{\mathrm{EC}} + (P_{\mathrm{EM}} Z_{\mathrm{EM}}) \circ S_{\mathrm{EM}}, \tag{2.14}$$

where $\circ$ is the convolution operator. The parameters Z_{EC}, Z_{EM}, S_{EC} and S_{EM} are calibrated and tabulated individually for each cell. Additional details on calibration can be found in section 2.8.2.

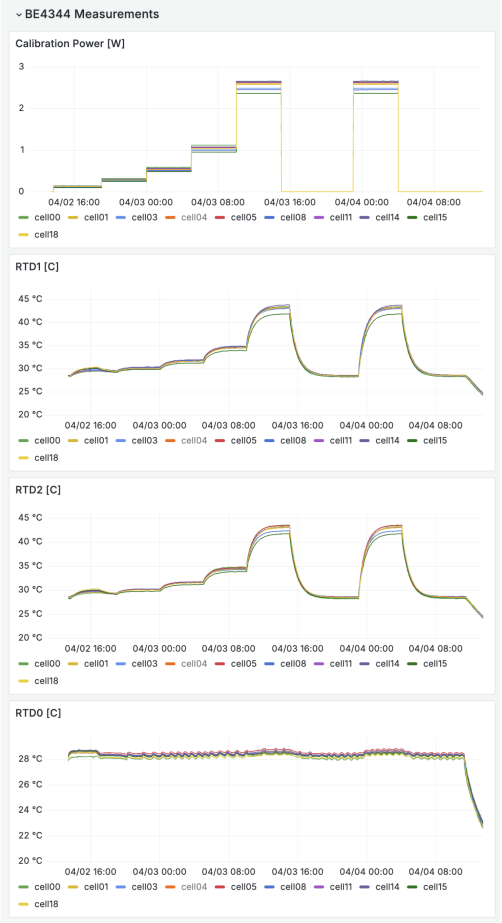

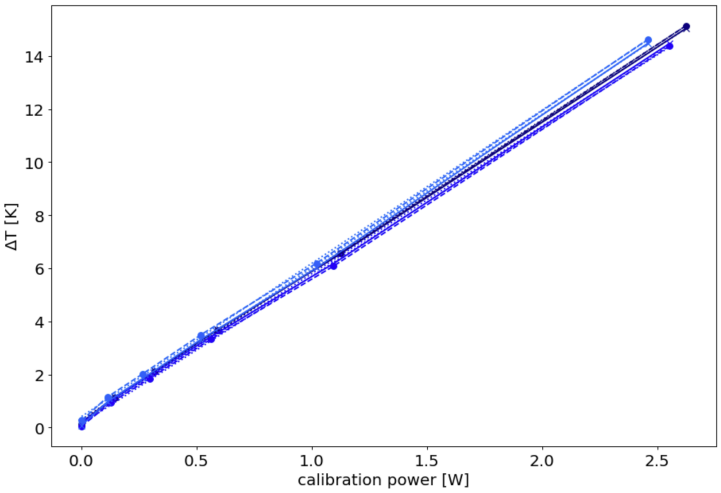

cell	RTD1 offset [K]	RTD1 linear [K/W]	RTD1 R2	RTD2 offset [K]	RTD2 linear [K/W]	RTD2 R2
00	0.293430	5.617317	0.999827	0.243105	5.676249	0.999821
01	0.233890	5.561895	0.999693	0.138313	5.562052	0.999680
03	0.227363	5.787277	0.999591	0.409358	5.775344	0.999609
04	0.477407	5.492763	0.999578	0.464404	5.472777	0.999721
05	0.107149	5.568385	0.999772	0.160515	5.602619	0.999727
08	0.306723	5.943332	0.999237	0.199163	5.597781	0.999462
11	0.148925	5.579426	0.999749	0.171404	5.549331	0.999727
14	0.296407	5.603953	0.999303	0.081532	5.486755	0.999467
15	0.236423	5.574253	0.999149	0.125986	5.573934	0.998999
18	0.386301	5.632505	0.999132	0.342747	5.604380	0.999423

Fig. 2.13: Results from multi-step calibration. Left panel, from top to bottom, shows calibration input power steps, followed by the temperature response of the two RTDs in the electrolyte, followed by the temperature of the base plate. The top right panel shows that reactor sensitivity is linear with input power. The bottom right panel shows the raw gain (K/W) and offset (K) from calibration.

2.10.4.2 Calculating COP and Heat Flow

It should be noted that, in its current configuration, UHTP is functioning as a screening test. It is performing 100 concurrent experiments searching for potential AHE. The methods for the screening tests are outlined below. Experiments with positive signals would be replicated in the HTcal to confirm reproducibility, and would also be replicated in the MS80 calorimeter in order to more accurately quantify the amount of excess heat observed.

In the presence of excess heat, the electrolyte temperature will be greater than the expected temperature for a given input power. At this point, we can make our first COP computation. This calculation is based

on expected temperature rather than expected heat as is used in HTcal. We denote the difference by adding a subscript 'T' to the COP.

$$\mathrm{COP_T} = \frac{\Delta T_{\mathrm{measured}}}{\Delta T_{\mathrm{expected}}} \tag{2.15}$$

A $\mathrm{COP_T}$ significantly greater than 1 tells us that excess heat is present (and AHE might be occurring), but does not tell us how much excess power is being produced. The excess heat can be computed based on certain assumptions. Given a measured excess temperature, it can be converted to excess heat using the thermal impedance. We don't know the exact thermal impedance Z_x for an excess heat event, because we don't know its location. It might be occurring near the cathode, in which case Z_{EC} is a good approximation for Z_x. In general, for most scenarios, $Z_{\mathrm{EM}} \leq Z_x \leq Z_{\mathrm{EC}}$. This typically bounds the excess heat by ±10 %.

Assuming Z_x is the weighted average of Z_{EC} and Z_{EM} (weighted with the respective input powers), the excess heat, P_{excess}, follows as:

$$P_{\mathrm{excess}} = P_{\mathrm{in}}(\mathrm{COP_T} - 1). \tag{2.16}$$

More generally,

$$P_{\mathrm{excess}} = \frac{\Delta T_{\mathrm{measured}} - \Delta T_{\mathrm{expected}}}{Z_x} = \frac{\Delta T_{\mathrm{excess}}}{Z_x}. \tag{2.17}$$

2.10.4.3 Minimum Transient Detection Threshold

To determine the sensitivity of the calorimeters, a series of constant power pulses were applied to the calibration resistor (Fig. 2.14b). Pulses ranged in duration and magnitude from 1 mW for 1 min to 50 mW for 45 min. This test demonstrated that a 5 mW pulse for 5 min (1.5 J) could be detected. However, this test was done under ideal conditions, starting from equilibrium with no electrochemical or electromigration input power. 5 mW for 5 min would be below the noise floor (driven by diurnal swings and recombiner variations) of a typical experiment which operates between 650 mW and 5.6 W.

2.10.5 Loading Measurement

The change in resistance of a palladium wire can be correlated to the change in the amount of hydrogen loading. This resistance change is in the milliohm range on a milliohm sample, necessitating a sensitive four-wire measurement. Given space and power constraints of the UHTP system, it was designed to leverage the electromigration current to measure sample resistance. When electromigration current is not required, the electromigration power supply sends a four-second two-level current (600 mA and 300 mA) pulse every 60 seconds. These values are the minimum pulse size and duration to get an accurate resistance measurement while introducing the least amount of parasitic heat into the calorimeter.

When electromigration is required, UHTP uses 3.2 A / 2.8 A level changes around a 3 A electromigration current. This two-level measurement is made at the same 4 seconds per 60 seconds cadence. The two-level measurement is accounted for in the input power balance, but at ~1 mW, has little impact on the system.

It should be noted that a trade-off was made between accurately measuring sample resistance and accurately measuring the electromigration input power in the choice of the placement of the voltage sense wires. For accurate resistance measurements, voltage senses should be placed on the sample, whereas for accurate heat measurements, voltage senses should be placed at the thermal system boundary. Because accurate calorimetry is a priority and qualitative loading measurements are sufficient, voltage senses were placed at the thermal system boundary.

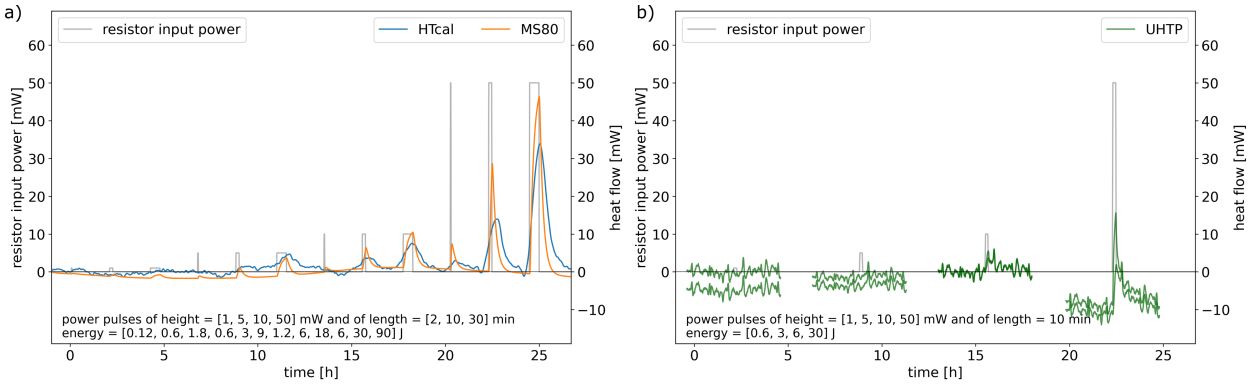

Fig. 2.14: Comparison of calorimeter heat flow responses to pulsed inputs in various calorimeters (MS80 and HTcal (a) and UHTP (b)). Note that all the pulses were applied consecutively in the MS80 and HTcal (a), but were assembled from different times in the UHTP (b). The two green lines in (b) represent the two temperature sensors in a given cell. Heat flows are shown for a single random cell per calorimeter, representing all cells.

2.11 Conclusion

The Setaram MS80 as well as the HTcal and the UHTP calorimeters should be more than sufficient to detect excess heat signals reported in the literature (Fig. 2.15). In contrast, we found that open system calorimetry is amenable to errors of similar magnitude as many reported excess heat measurements.

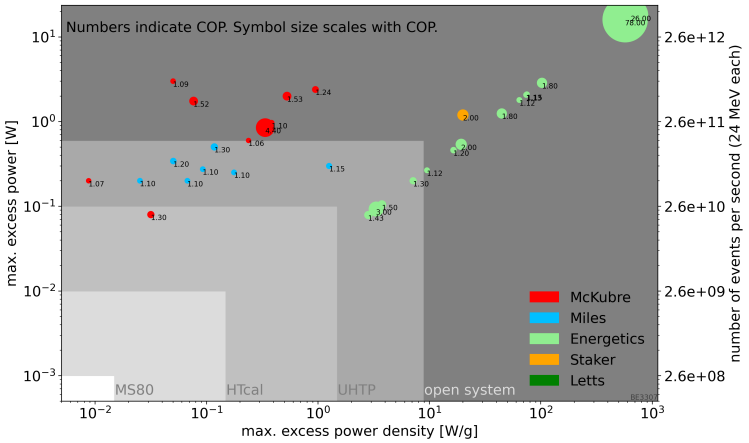

Fig. 2.15: Illustration of detection thresholds with our calorimeters (MS80, HTcal, UHTP, open system) calorimeters compared to excess heat reports in the literature. Note that the white space in the lower left is 'uncharted territory', not easily resolvable with our calorimeters.